Physica A 388 (2009) 2299–2305

Contents lists available at ScienceDirect

Physica A

journal homepage: www.elsevier.com/locate/physa

Threshold-diversity-induced resonance

Hanshuang Chen [a,*], Zhonghuai Hou [a,b], Houwen Xin [a]

[a] Department of Chemical Physics, University of Science and Technology of China, Hefei, Anhui, 230026, People's Republic of China

[b] Hefei National Laboratory for Physical Sciences at Microscale, University of Science and Technology of China, Hefei, Anhui, 230026, People's Republic of China

ARTICLE INFO

Article history:
Received 12 December 2008
Received in revised form 17 February 2009
Available online 26 February 2009

PACS:
05.40.Ca
05.45.-a
89.75.-k

Keywords:
Diversity
Stochastic resonance
Noise
Complex network

ABSTRACT

The effect of diversity on a system of coupled threshold elements is investigated, where each element is driven by a common periodic signal. Diversity is introduced to the system by assuming that the thresholds of all units are heterogeneous, e.g. the thresholds follow a Gaussian or other distribution. A combined numerical and analytical approach shows that the response of the system to the input signal is maximized at a moderate value of the diversity amplitude, which is similar to the well-known stochastic resonance phenomenon induced by noise. Our findings exhibit that the diversity, a kind of spatial disorder, may play a similar role to noise as a kind of temporal disorder.

1. Introduction

Stochastic resonance (SR) is a well-known phenomenon where noise enhances the response to weak periodic driving, as observed in many different physical, chemical and biological systems [1–3]. Over the last two decades, studies of the SR phenomenon in nonlinear dynamical systems composed of many coupled identical units have attracted great research interest. One of the most interesting phenomena is array-enhanced stochastic resonance, where the response of a bistable noisy oscillator to an external periodic signal is further optimized by coupling it locally to an array of identical oscillators [4].

However, the assumption of identical units is not very realistic for many natural systems. For instance, in biochemical systems the intrinsic frequencies of biochemical oscillators are usually not identical: the cellular structure and function are generally various. Taking into account social systems, individual differences usually result from emotional factors, social status, etc. This issue usually implies that the units composing the ensemble present some disparities in the values of one or more characteristic parameters, and this has attracted much attention recently. For instance, Braiman et al. have shown that diversity can enhance synchronization in an array of Josephson junctions [5]. Mousseau has demonstrated that the introduction of disorder can synchronize an integrate-and-fire coupled-map earthquake model [6]. Lindner et al. have shown that an optimal magnitude of disorder, induced by the disparity of the pendulum lengths in an array of coupled pendulums, can order spatiotemporal chaos [7]. Zhou et al. have found that the inhomogeneity in the parameters of array-coupled FitzHugh–Nagumo (FHN) oscillators dramatically enhances the coherence [8]. More interestingly, Tessone et al. reported very recently that diversity could induce a resonant collective behavior in an ensemble of coupled bistable or excitable systems [9]. This phenomenon is called diversity-induced resonance, similar to well-known SR where resonance is induced by noise. Gassel et al. considered coupled forced FHN oscillators, and achieved the optimal enhancement of the signal by

* Corresponding author.
E-mail addresses: chenhshf@mail.ustc.edu.cn (H. Chen), hzhlj@ustc.edu.cn (Z. Hou).

0378-4371/$ – see front matter © 2009 Elsevier B.V. All rights reserved.
doi:10.1016/j.physa.2009.02.024

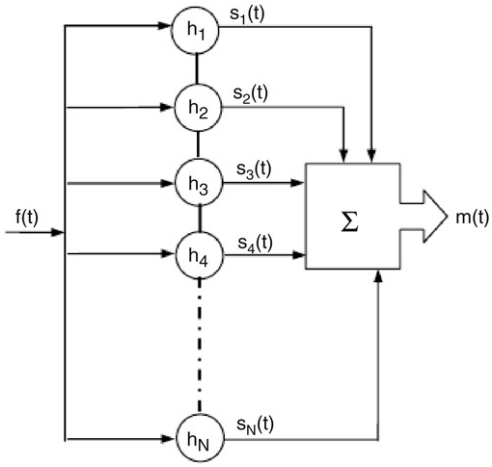

Fig. 1. A schematic representation of N coupled threshold elements. Each element is subject to a common external signal, but their thresholds are heterogeneous.

both additive and multiplicative diversities (double-diversity-induced resonance) [10]. Some diversity-related effects have also been reported in many other papers, and these findings have shown that diversity could induce pattern formation in excitable media [11], could enhance cellular ability to detect sub-threshold extracellular signals [12], could enhance the time precision of firing in a neural network [13], might provide a possibility for the control of chaos in spatially extended chaotic systems [14], etc. [15,16].

In the present work we consider a model of N coupled threshold elements, each unit of which takes one of two possible states, 0 and 1. The state of each unit is decided by the states of its nearest neighbors as well as an external signal. In particular, the thresholds of the elements are heterogeneous, and we are interested in the effects of this kind of threshold diversity. This model is a simple paradigm for many real systems. A common situation is that of the existence of a rest state and an excited state for many biological systems such as a neuron, where the two states are separated via a threshold [1,17,18]. In such systems, all units vary in their size, shape, etc., such that the dynamical thresholds of subsystems are usually heterogeneous. Another notable example is that two states represent agreement and disagreement about a topic, respectively. In this case, each individual has one of the two opinions, which is not only affected by the ambient majority's opinion, but is also dependent on his own preference [19]. This preference is often modeled by a parameter regarded as an opinion threshold that defers from one opinion to another. Therefore, the present model is a general representation of many real systems and the consideration of threshold diversity is of realistic importance. To this end, we introduce threshold diversity by assuming that the threshold follows a Gaussian or other distribution. It is found that the response of the system to the input signal exhibits resonant dependence on the diversity. We support our finding by numerical simulation and theoretical analysis.

2. Model description

We consider a model of N coupled threshold elements, where the state of each element can adopt one of two possible values, $s_i = 0$ or $s_i = 1$. This value is updated according to the following rule [20]:

$$s_i(t+1) = \begin{cases} \Theta\left(\sum_{j\in\Omega_i} s_j(t) - h_i\right), & \text{w.p. } 1 - |f(t)| \\ \Theta\left(f(t)\right), & \text{w.p. } |f(t)| \end{cases} \tag{1}$$

where w.p. denotes 'with probability', Ω_i is the set of all neighbors of node i, and $\Theta(\cdot)$ is the Heaviside step function. $f(t) = A\sin(\omega t)$, where A and ω are the amplitude and frequency of the input signal, respectively. h_i is the threshold of node i. A schematic representation of the model is exhibited in Fig. 1.

Our aim is general, due to the model being able to have its significance interpreted from many different points of view. For instance, in the social field the two states can represent two opposite opinions, and the coupling term denotes the majority rule [21], while an individual's preference to one of the two opinions can be regarded as a threshold, and the effect of external surroundings, for example advertisements, can be prescribed by a harmonic signal. In many biochemical networks the two states can represent a neuron being fired or not, or a gene being expressed or not, and the coupling term denotes the received signals from the whole neighborhood; the threshold is an excitable separation of the two states, and the external stimulation is usually modeled by a periodic signal. Threshold diversity is introduced by assuming that the threshold parameter h_i obeys a Gaussian distribution satisfying $\langle h_i\rangle = \langle h\rangle$ and $\langle (h_i - \langle h\rangle)(h_j - \langle h\rangle)\rangle = \sigma_g^2\delta_{ij}$, where σ_g is the

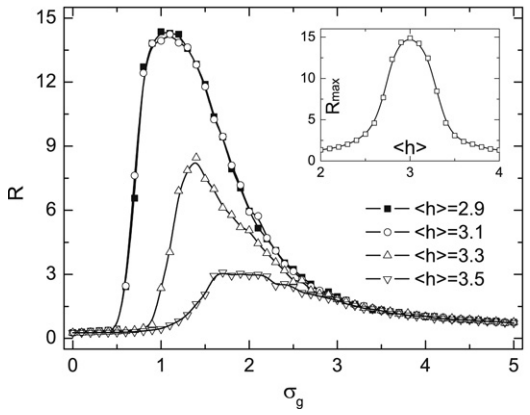

Fig. 2. Dependences of R on the diversity σ_g for different $\langle h\rangle$. The inset depicts the dependence of $R_{\max}$ on $\langle h\rangle$. The other parameters are $N = 1000$, $K = 6$, $A = 0.15$, and $\omega = 2\pi/128$.

standard deviation measuring the magnitude of the diversity. To quantify the response of the system to the input signal, we calculate the spectral amplification factor R, defined as the ratio of the output to input power at the corresponding driving frequency, [22]

$$R = \left\langle \frac{4}{A^2} \left| \langle\langle m(t) e^{-i\omega t} \rangle\rangle \right| \right\rangle, \tag{2}$$

where $m(t) = N^{-1}\sum_{i=1}^{N} s_i(t)$ is the mean field. $\langle\langle\cdots\rangle\rangle$ and $\langle\cdots\rangle$ denote the average over time and initial conditions, respectively. Numerical simulations are carried out by using synchronous updating. At each run, the first 10^4 time steps are discarded to achieve a steady state and the following 10^4 time steps are used to investigate the system's dynamics. We also performed extensive numerical calculations by using asynchronous updating and found that the following results are essentially consistent with those when using synchronous updating.

3. Numerical results

We start from homogeneous random networks, where each node is randomly connected to K neighbors from the whole networks. Each node is randomly assigned an initial state $s(0) = 0$ or $s(0) = 1$ with equal probability $1/2$. The dependences of R on the diversity σ_g for different $\langle h\rangle$ are depicted in Fig. 2 with relevant parameters $N = 1000$, $K = 6$, $A = 0.15$, and $\omega = 2\pi/128$. Here the amplitude of the input signal is set to be sub-threshold, i.e. without diversity the response of the system to the signal is very faint. Each piece of data is the result of averaging over 20 different initial conditions. With an increment of σ_g, R reaches a maximum $R = R_{\max}$ and then decreases as σ_g increases further. Thus, there exists an optimal σ_g for the maximal R, indicating the occurrence of *threshold-diversity-induced resonance*. Furthermore, the location and the amplitude of the resonant peak are relevant to the mean value of the threshold $\langle h\rangle$. As $\langle h\rangle$ increases from $\langle h\rangle = 3$, the location of the resonant peak shifts right and the height of the resonant peak becomes lower and lower. In the other direction, that is, as $\langle h\rangle$ decreases from $\langle h\rangle = 3$, similar phenomena will occur. As a direct demonstration, the comparisons between two curves for $\langle h\rangle = 2.9$ and $\langle h\rangle = 3.1$ are drawn, and one can clearly find that the two curves almost overlap. The inset depicts $R_{\max}$ as a function of $\langle h\rangle$ and we find $R_{\max}$ is maximal at $\langle h\rangle = 3$. When the input signal and threshold diversity are both absent, the states of all nodes will become identical with the time increment, i.e. $s(\infty) = 0$ or $s(\infty) = 1$ for any node depending on the threshold h. Concretely, $s(\infty) = 1$ is reached for $h \leqslant 3$ and $s(\infty) = 0$ for $h > 3$, which is analyzed in detail in next section. A key point is that the average threshold $\langle h\rangle$ is set to around $\langle h\rangle = 3$ such that the resonance phenomenon is clearly exhibited.

This phenomenon can be explicitly seen by observing the time evolution of the mean field m as shown in Fig. 3. One can notice that, on the one hand, m oscillates in time with the frequency of the input signal ω; on the other hand, the oscillatory fashions are different for different σ_g. For small σ_g, m oscillates around the value zero (or one when $\langle h\rangle < 3$) with the amplitude close to that of the input signal A. As σ_g is increased, both the amplitude and the center value of the oscillation dramatically increase. When σ_g increases again, the amplitude of the oscillation decreases but the center value of the oscillation increases. We give a qualitative explanation of above phenomenon from a microscopic point of view. When the diversity σ_g is very small, all nodes are below the dynamical threshold. In this case the external signal dominates all nodes such that $m(t) = |A\sin\omega t|\,\Theta(\sin\omega t)$. If σ_g is very large, about half of the nodes are below the dynamical threshold and the other half are above the threshold. Furthermore, a majority of nodes are far from their threshold and thus few nodes can switch between being above and below the threshold. In this case $m(t) = \frac{1}{2} + \frac{1}{2}A\sin\omega t$ such that the signal is not amplified. For a moderate value of σ_g, the numbers of nodes above and below the threshold are comparative, and all the nodes locate near the threshold. It is possible that the sub-threshold nodes become supra-threshold, especially when the

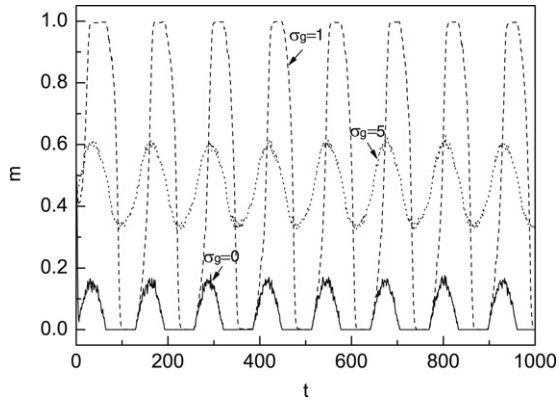

Fig. 3. Typical time evolution of m for different σ_g. The other parameters are $N = 1000$, $K = 6$, $\langle h \rangle = 3.1$, $A = 0.15$, and $\omega = 2\pi/128$.

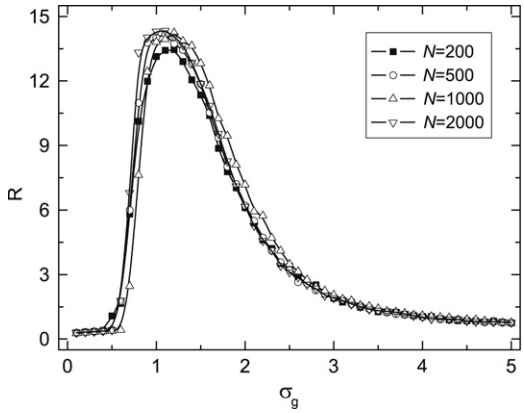

Fig. 4. Dependences of R on the diversity σ_g for different numbers of elements N. The other parameters are $K = 6$, $\langle h \rangle = 3.1$, $A = 0.15$, and $\omega = 2\pi/128$.

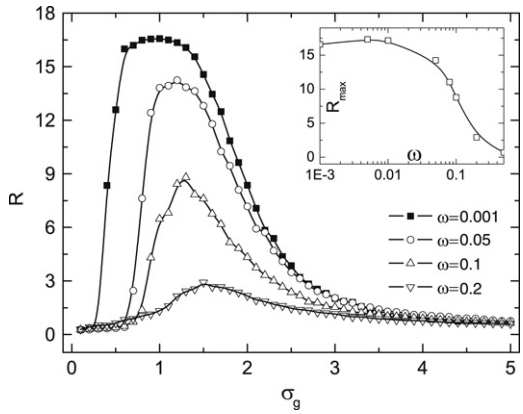

Fig. 5. Dependences of R on the diversity σ_g for different frequencies of the input signal ω. The inset depicts the dependence of $R_{\max}$ on ω. The other parameters are $N = 1000$, $K = 6$, $\langle h \rangle = 3.1$, and $A = 0.15$.

input signal is positive. Once this situation occurs, more and more nodes cross the threshold from below due to a positive feedback mechanism. When the input signal is negative, the opposite process takes place. Therefore the mean field can oscillate with large amplitude, resulting in the amplification of the signal.

We now consider the effects of the number of units N and the frequency of the input signal ω on the resonant behavior in coupled threshold elements. In Fig. 4, the dependences of R on σ_g for different N are exhibited. One can notice that the location and height of the resonant peak do not depend on the number of units. In Fig. 5, the dependences of R on σ_g for different frequencies of the input signal ω are shown. As ω is increased, the maximal R decreases and the optimal σ_g for the maximal R shifts to a larger value.

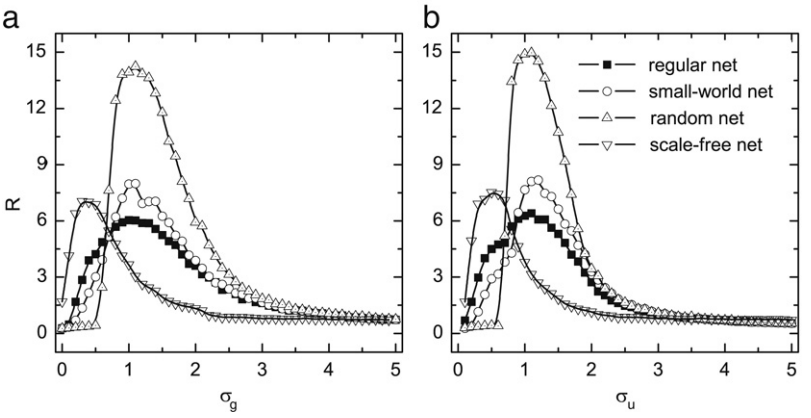

Fig. 6. R as a function of the diversity for different distributions of threshold and different types of network. The left panel and right panel correspond to a Gaussian distribution and a uniform distribution, respectively. The other parameters are $N = 1000$, $K = 6$, $\langle h\rangle = 3.1$, $A = 0.15$, and $\omega = 2\pi/128$.

To make a comparative study between different distributions of thresholds, we investigate an alternative shape of distribution, e.g. a uniform distribution in which the parameter h_i is randomly selected in the range $[\langle h\rangle - \delta, \langle h\rangle + \delta]$, where the standard deviation $\sigma_u = \delta/\sqrt{3}$ is the magnitude of the diversity.

In addition, we compare the numerical results on different network types: regular network, small-world network, random network and scale-free network. We here consider a homogeneous small-world network, which is generated by starting from an undirected regular graph with size $N = 1000$ and average degree $K = 6$; a two-step circular procedure is introduced: (i) choose two different edges randomly, which have not been used yet in step (ii) and (ii) swap the ends of the two edges [23]. Duplicate connections and disconnected graphs are prohibited. A dimensionless parameter p, which denotes the fraction of swapped edges in the network, is introduced: $p = 0$ corresponds to a regular network, whereas $p = 1$ corresponds to a homogeneous random network. For $p = 0.2$, the resulting network has the features of small-world network characterized by short average path length and high clustering coefficient. In contrast to the Watts–Strogatz model [24], this network has small-world effect together with keeping the degree of each node unchanged. A scale-free network is generated via growth and preferential attachment as proposed by Barabási and Albert [25], again comprising $N = 1000$ nodes and having average degree $K = 6$. Since the degree distribution of such a network follows a power law with an exponent equaling -3, the degree heterogeneity of nodes is substantial. In Fig. 6 the dependences of R on the diversity with the two shapes of distributions and the four network types are shown. Whether we apply a Gaussian distribution or a uniform distribution, whether we use a random network or other networks, the numerical results indicate that the resonant phenomenon always appears. Moreover, the locations of the resonant peaks are almost unaffected by the shapes of distributions. The resonant peaks for the scale-free network locate to the left of those for the other three networks. On the other hand, the heights of the resonant peaks for the uniform distribution are slightly larger than for the Gaussian distribution, while the resonant peaks for the random network are much higher than those for the other types of network.

4. Mean field analysis

In this part, we present a theoretical analysis from the view of the mean field. We first consider the case that the input signal is absent and the threshold is homogenous, and thus the evolution equation for m is given by

$$\begin{aligned}\frac{\mathrm{d}m}{\mathrm{d}t} &= (1-m)\Pr(0\to 1) - m\Pr ob(1\to 0)\\ &= -m + \Pr(0\to 1),\end{aligned} \tag{3}$$

where $\Pr(0\to 1)$ is the probability that the node in state 0 changes its state, which can be readily written as

$$\Pr(0\to 1) = \Pr(Km \geqslant h). \tag{4}$$

One can calculate the above expression by the cumulative probability function of the binomial distribution

$$\Pr(Km \geqslant h) = \sum_{x=\lceil h\rceil}^{K} \frac{K!}{x!\,(K-x)!} m^x (1-m)^{K-x}, \tag{5}$$

where $\lceil\cdot\rceil$ is the ceiling function. Assuming the initial value $m = 0.5$, the stable solution of Eq. (3) is $m = 1$ for $h \leqslant K/2$ and $m = 0$ for $h > K/2$. Thus the transition point of the two stable states occurs at $h = K/2$.

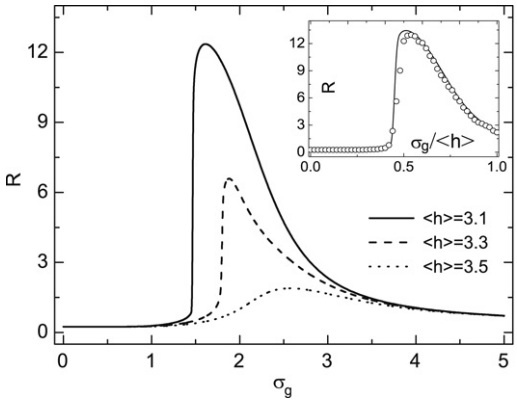

Fig. 7. Results of theoretical analysis: dependences of R on the diversity σ_g for different $\langle h\rangle$. The other parameters are $K = 6, A = 0.15$, and $\omega = 2\pi/128$. The inset depicts the dependences of R obtained from numerical calculations (symbol) and analytical results (continuous line) on the diversity in a globally coupled network.

For the case of a heterogeneous threshold, $\Pr(Km \geqslant h)$ can be replaced with $\Pr(Km \geqslant h_i)$. If the threshold satisfies the Gaussian distribution considered in the above section, $\Pr(Km \geqslant h_i)$ can be calculated by the cumulative probability function of the Gaussian distribution, and thus the rate equation of Eq. (3) is rewritten as

$$\begin{aligned}\frac{\mathrm{d}m}{\mathrm{d}t} &= -m + \Pr(Km \geqslant h_i) \\ &= -m + \frac{1}{2}\left(1 + \mathrm{erf}\left(\frac{Km - \langle h\rangle}{\sigma_g\sqrt{2}}\right)\right),\end{aligned} \tag{6}$$

where $\mathrm{erf}(\cdot)$ is the error function, and $\langle h\rangle$ and σ_g are the mean value and the standard deviation of the threshold, respectively. When σ_g is very large, the error function is very close to zero and thus the mean field $m \to 0.5$. We now add the input signal to Eq. (6), which yields

$$\frac{\mathrm{d}m}{\mathrm{d}t} = -m + (1 - |A\sin(\omega t)|)\Pr(Km \geqslant h_i) + |A\sin(\omega t)|\,\Theta(\sin\omega t). \tag{7}$$

The time evolution of m is obtained via the numerical integration of Eq. (7), and we then calculate the spectral amplification factor R. The mean-field results of the dependences of R on σ_g for different $\langle h\rangle$ are shown in Fig. 6. It is clear that the results of the theoretical analysis correctly predict the trends that R changes with σ_g and $\langle h\rangle$. Quantitatively speaking, the height of the resonant peak in the random network is slightly higher than the analytical result, while that in the other networks is obvious lower than the analytical result. Regarding the location of the resonant peak, the analytical results are more right than the numerical results in all considered networks. One can expect that the theoretical analysis agrees well with numerical calculations in a globally coupled network due to the global network satisfying a well-mixed condition. To this end, the comparison is shown in the inset of Fig. 7 between the dependence of R on σ_g, the diversity obtained from numerical calculations and the theoretical analysis in a global network of $N = 1000$ coupled elements, where they show excellent agreement. The above theoretical treatment is also practical if the threshold satisfies a uniform distribution. In this case the last term on the right-hand side of Eq. (6) can be replaced by the cumulative probability function of the uniform distribution. We also perform a comparative study between numerical calculations and the theoretical analysis, where both results are also qualitatively satisfied.

5. Conclusions

In summary, we have investigated numerically and analytically the influence of the threshold diversity on the dynamics of coupled threshold elements. It was found that the diversity can induce resonance-like behavior, which is similar to the well-known stochastic resonance induced by noise. Numerical and theoretical results showed good agreements, regarding the resonance behavior as well as the dependences of the location of the peak on the mean value of the threshold. It was not surprising that the numerical results in a random network better fit theoretical analysis than those in a regular network, e.g. the height of the resonant peak due to a random network better supports the well-mixed condition. We have considered two kinds of ordinary distribution, a Gaussian distribution and a uniform distribution, and found that no matter which kind of distribution is applied to the threshold the resonant phenomenon robustly appears; moreover, the location of the peak is not sensitive to the diversity and the height of the peak is also almost unaffected by the shape of the distributions. Since network heterogeneity usually mingles with other disorder, we have performed a numerical study in a regular network to

eliminate the effect of connectivity randomness. It was found that the dependence of R on the diversity also exhibits a non-monotonic behavior. Indeed, it is obvious that network randomness enhances the resonant behavior by comparing the height of the resonant peaks between a random network and a regular network. However, network randomness is not an absolutely necessary condition of the occurrence of the present resonant behavior. It is worth mentioning that the Gaussian distribution threshold h_i referred to here is different from adding Gaussian white noise to the homogeneous threshold $h_i = \langle h \rangle + \xi_i(t)$, where $\xi_i(t)$ satisfies $\langle \xi_i(t) \rangle = 0$ and $\xi_i(t)\xi_j(t') = \sigma^2 \delta_{ij} \delta(t - t')$. The threshold diversity represents quenched randomness, i.e. the threshold varies with space but it does not evolve with time denoted by a kind of spatial disorder.

Our findings have indicated that an appropriate level of diversity, as many other types of disorder, could improve the response of the system to the input signal. Such a resonant effect renders us to speculate that the right amount of diversity present in some biological systems has an important function. In the course of long-term evolution, the right amount of diversity might be self-tuned to enhance the detection of weak signals in these biological systems. We also hope that this work fosters experimental research in this direction.

Acknowledgement

This work was supported by the National Science Foundation of China (Grants No. 20673106).

References

[1] L. Gammaitoni, P. Hänggi, P. Jung, F. Marchesoni, Rev. Modern Phys. 70 (1998) 223–287;
B. Lindner, J. Garcia-Ojalvo, A. Neiman, L. Schimansky-Geier, Phys. Rep. 392 (2004) 321–424;
F. Sagué, J.M. Sancho, J. García-Ojalvo, Rev. Modern Phys. 79 (2007) 829–882.
[2] J.J. Collins, C.C. Chow, T.T. Imhoff, Nature 376 (1995) 236–238.
[3] N.G. Stocks, Phys. Rev. Lett. 84 (2000) 2310–2313.
[4] J.F. Lindner, B.K. Meadows, W.L. Ditto, et al., Phys. Rev. Lett. 75 (1995) 3–6; Phys. Rev. E 53 (1996) 2081–2086.
[5] Y. Braiman, W.L. Ditto, K. Wiesenfeld, M.L. Spano, Phys. Lett. A 206 (1995) 54–60.
[6] N. Mousseau, Phys. Rev. Lett. 77 (1996) 968–971.
[7] J.F. Lindner, B.S. Prusha, K.E. Clay, Phys. Lett. A 231 (1997) 164–172;
F. Qi, Z.H. Hou, H.W. Xin, Phys. Lett. A 308 (2003) 405–410.
[8] C.S. Zhou, J. Kurths, B. Hu, Phys. Rev. Lett. 87 (2001) 098101.
[9] C.J. Tessone, C.R. Mirasso, R. Toral, J.D. Gunton, Phys. Rev. Lett. 97 (2006) 194101.
[10] M. Gassel, E. Glatt, F. Kaiser, Phys. Rev. E 76 (2007) 016203.
[11] E. Glatt, M. Gassel, F. Kaiser, Phys. Rev. E 75 (2007) 026206; Europhys. Lett. 81 (2008) 40004.
[12] H.S. Chen, J.Q. Zhang, J.Q. Liu, Phys. Rev. E 75 (2007) 041910.
[13] H.S. Chen, J.Q. Zhang, J.Q. Liu, Physica A 387 (2008) 1071–1076.
[14] H.S. Chen, J.Q. Zhang, Phys. Rev. E 77 (2008) 026207.
[15] M. Perc, A. Szolnoki, Phys. Rev. E 77 (2008) 011904;
A. Szolnoki, M. Perc, G. Szabó, Eur. Phys. J. B 61 (2008) 505–509;
T.V. Martins, R. Toral, M.A. Santos, arXiv:0805.4501.
[16] R. Toral, E. Hernández-García, J.D. Gunton, arXiv:0806.2106.
[17] J.K. Douglass, L.A. Wilkens, E. Pantazelou, F. Moss, Nature 365 (1993) 337–340.
[18] J.J. Collins, T.T. Imhoff, P. Grigg, J. Neurophysiol. 76 (1996) 642–645.
[19] P. Klimek, R. Lambiotte, S. Thurner, Europhys. Lett. 82 (2008) 28008.
[20] M. Kuperman, D. Zanette, Eur. Phys. J. B 26 (2002) 387–391;
A. Krawiecki, Physica A 333 (2004) 505–515;
C.J. Tessone, R. Toral, Physica A 351 (2005) 106–116.
[21] C. Castellano, S. Fortunato, V. Loreto, arXiv:0710.3256.
[22] P. Jung, P. Hänggi, Europhys. Lett. 8 (1989) 505–510.
[23] F.C. Santos, J.F. Rodrigues, J.M. Pacheco, Phys. Rev. E 72 (2005) 056128.
[24] D.J. Watts, S.H. Strogatz, Nature 393 (1998) 440.
[25] A.-L. Barabási, R. Albert, Science 286 (1999) 509.